11th World Congress on Computational Mechanics (WCCM XI)
5th European Conference on Computational Mechanics (ECCM V)
6th European Conference on Computational Fluid Dynamics (ECFD VI)
E. Oñate, J. Oliver and A. Huerta (Eds)

THE PHYSICS OF STARTING PROCESS FOR VERTICAL AXIS WIND TURBINES

HORIA DUMITRESCU[*], VLADIMIR CARDOŞ[*] AND ION MĂLĂEL[†]

[*] "Gh. Mihoc - C. Iacob", Institute of Mathematical Statistics and Applied Mathematics Calea 13 Septembrie 13 Bucharest 050711, Romania
e-mail: horiadumitrescu@yahoo.com, www.ima.ro

[†] COMOTI National Research & Development for Gas Turbines – Bucharest
email: ion.malael@comoti.ro

Key Words: *Dynamic stall, Low Reynolds number, Aerodynamics, VAWT, Renewable energy*

Abstract. In urban areas the wind is very turbulent and unstable with fast changes in direction and velocity. In these environments, the use of small vertical axis wind turbines (VAWT) becomes increasingly attractive due to several advantages over horizontal axis wind turbines (HAWT). However, such designs have received much less attention than the more common propeller-type designs and the understanding of same aspects of their operation remains, to this day, incomplete. This is particularly true of their starting characteristics. Indeed, same authors heuristically maintain that they cannot start without external assistance. This paper reviews the cause of the inability of the low solidity fixed pitch vertical axis wind turbines to self start, and investigates the way of overcoming this draw back.

1 INTRODUCTION

Traditionally, wind turbine performance is defined in terms of power-extraction performance (expressed dimensionless as power coefficient, C_p) and the turbine's ability to start is normally ignored. Nevertheless if a turbine cannot accelerate through start-up, its power-extraction performance is drastically limited. The consideration of starting behavior therefore offers another solution to improve the overall performance as the period that the turbine needs to start might be shortened and a longer power-production period might be achieved. Therefore, it is crucial on to have a good understanding of the mechanism of start, in particular at relatively low Reynolds number ($\mathrm{Re}_c \cong 10^5$) appropriate to the urban applications. Different types of wind turbines behave differently during start up. In present paper particular attention is paid to vertical axis wind turbines (VAWT) which are not fully understood.

2 AERODYNAMICS OF A VAWT

The movement of the blades in a VAWT entails a large range of flow regimes from rest to the operating condition. In order to understand the starting behavior, it is useful to consider flow conditions experienced by the turbine blade when it rotates around its vertical axis.

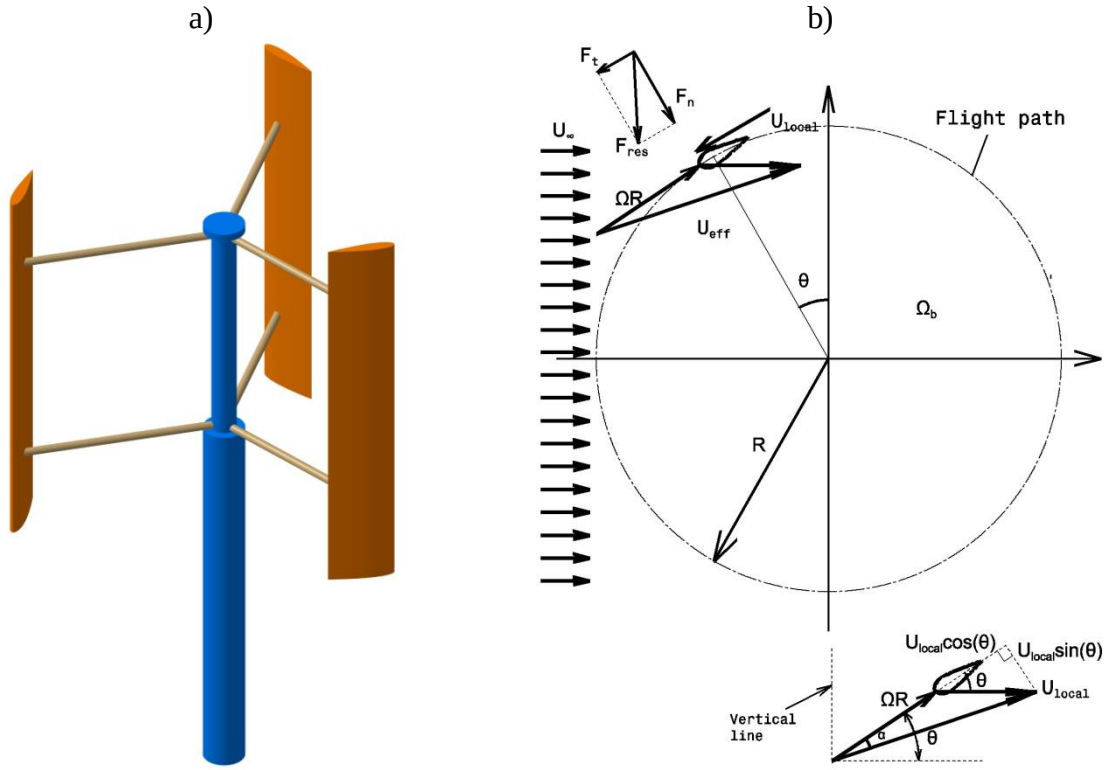

Figure 1: Basics of VAWT: a) sketch of a fixed-pitch straight-bladed VAWT; b) typical flow velocities in Darrieus motion.

Figure 1a is a schematic of a straight-bladed-fixed-pitch VAWT which is the simplest, but typical form, of the Darrieus type VAWTs. Despite the simplicity, its aerodynamic analysis is still quite complex. One feature is that the relative velocities perceived by the blade always change as the blade moves at different azimuthal positions. Figure 1b illustrates typical flow velocities around a rotating VAWT blade at a given azimuthal angle θ, as well as the aerodynamic forces perceived by the blade. The azimuthal angle θ is set to be zero when the blade is at the top of the flight path and is increases in a counter-clockwise direction. It should be noted that, even neglecting the variation of the induced local flow velocity, U_{local} both the magnitude and the direction of the effective velocity perceived by the blade, U_{eff}, change in a cyclic manner as the blade rotates through different azimuthal angles. This kind of motion is called the Darrieus motion [1]. As a result, the aerodynamic loads exerted on the blade change cyclically with θ.

From the vectorial description of velocities, Fig. 1b, we can obtain the following expression that establishes the relationship between the angle of attack α_D, the tip speed ratio (TSR) λ and the azimuthal angle θ of a blade in Darrieus motion (without velocity induction)

$$\tan\alpha_D = \frac{U_\infty \sin\theta}{\Omega R + U_\infty \cos\theta} = \frac{\sin\theta}{\lambda + \cos\theta} \; or \; \alpha = \arctan\left(\frac{\sin\theta}{\lambda + \cos\theta}\right), \tag{1}$$

Another important parameter is the reduced frequency which governs the level of unsteadiness.

The reduced frequency *k*, defined as $k = \omega c / 2U_{eff}$, where ω is the angular frequency of the unsteadiness, *c* is the blade chord and U_{eff} is the velocity of the blade, can be expressed in terms of TSR as

$$k = \left(\frac{c}{D}\right)\frac{\lambda}{\sqrt{\lambda^2 + 2\lambda\cos\theta + 1}}, \tag{2}$$

The variation of angle of attack α_D, its normalized values $\alpha_D / \alpha_{D\max}$, and the reduced frequency are evaluated from Eqs (1) and (2) as functions of the azimuthal angle θ for various values of λ, as shown in Fig. 2.

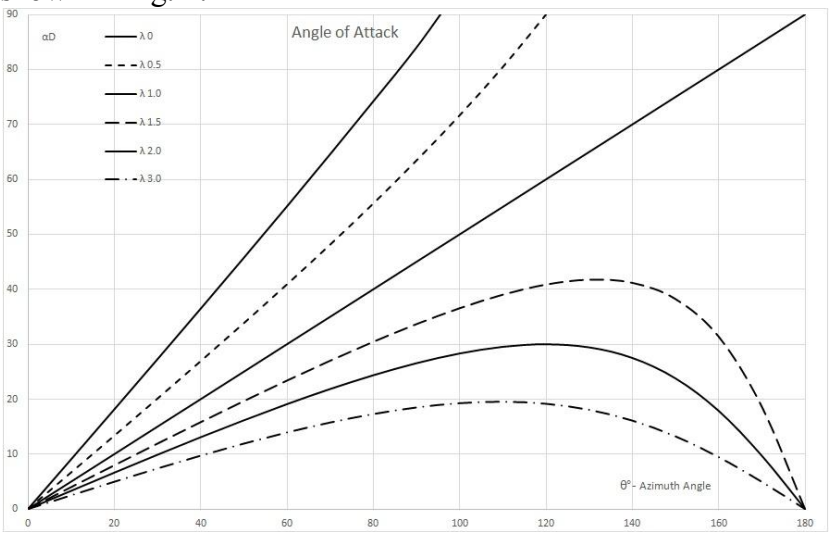

a)

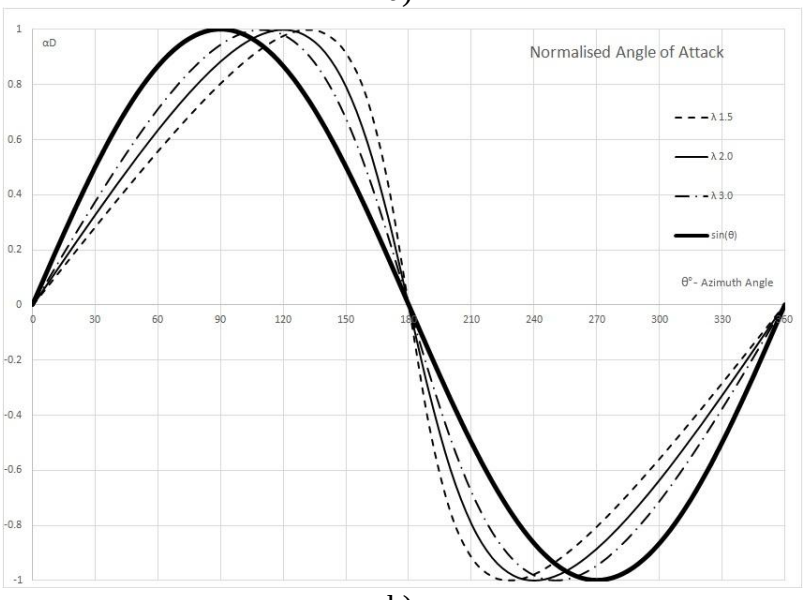

b)

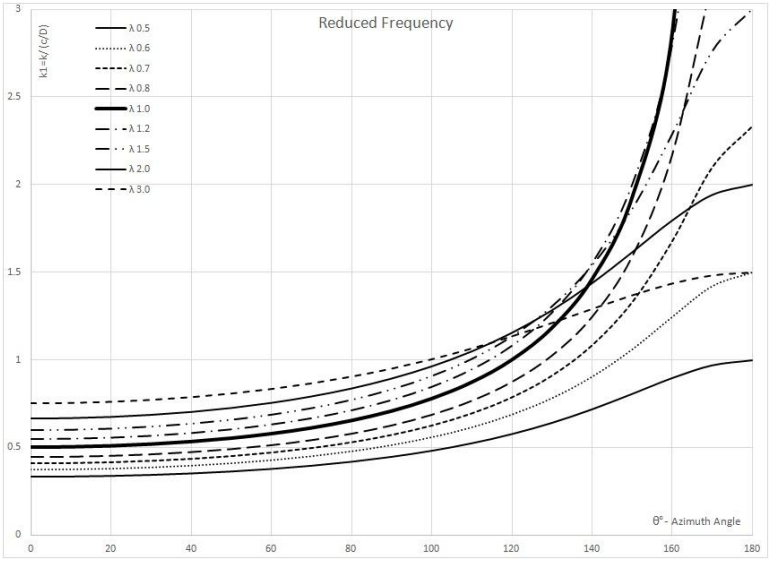

c)

Figure 2: Flow conditions for Darrieus blade: a) variation of angle of attack; b) normalized angle of attack and sine–curve; c) reduced frequency as a function of λ and the azimuth angle θ.

This figure shows some specific features of the Darrieus motion which behavior differently in terms on TSR as:

- The variation of angle of attack for $\lambda \approx 1$ presents a strong discontinuity type instability in the point of maximum incidence corresponding to the change of incidence direction at the downstream passage ($\theta = 180^0$); for the values $\lambda > 1$, the passage point is a inflectional instability of incidence variation when the angle of attack becomes zero, (Fig. 2a). The unsteady flow phenomena caused by the instabilities of Darrieus motion are complex mechanism involving the formation of an intense leading-edge vortex, post-stall vortex shedding, rotational circulation, and wake capture.
- The variations of normalized angles of attack α at the high values of λ ($\lambda \geq 2$) are very similar to the sine-curve, i.e. $\alpha = \sin\theta$ with their peaks at about same azimuthal angle of 90^0; unlike these variations, the variations at the low values of λ (λ<2) contain elements of plunging motion with their peaks at different azimuth angles (130^0 for λ=1.5), Fig 2b. This difference is typically termed the phase shift which is an important parameter for generation of thrust.
- The variation of the reduced frequency *k* shows the existence of a band of tip speed ratios about λ ≈ (0.7-1.5) with the rough increase of frequency like a discontinuity (Fig. 2c).

According to the diagram from Fig. 2c the unsteadiness associated with the flow field and VAWT operating state can be classified into three levels:

- Zero level is the distributed unsteadiness, when $k/(c/D) \leq 1.0$ and λ ≤ 0.5; commonly its effect is neglected and a quasi-steady assumption is used;

- First level is the located unsteady phenomenon of dynamic stall with lift increment at low angle of attack ($\alpha \approx 25^0$),occurring at $\theta=90^0$ when $k/(c/D) \le 2.0$ and $\lambda \ge 2$; its effect is similar to a sinusoidal pitching airfoil;
- Second level is a located unsteady phenomenon of dynamic stall with drag reduction at high angle of attack ($\alpha > 45^0$), occurring at $\theta=180^0$ when $k/(c/D) > 2.0$ and $\lambda \cong 0.7-1.5$; to this day it is still unknown.

The two types of dynamic stall address to different portions of the static lift characteristic which for the VAWT blades operating at low TSR presents a particular double stall behavior with two stall values, $C_{L_{1SS}}$ at low AOA and $C_{L_{2SS}}$ at high AOA, (Fig. 3). The main difference between these two types of stall is dependence upon the Reynolds number: first stall is much dependent on Reynolds number and second stall is practically with no-effect on it.

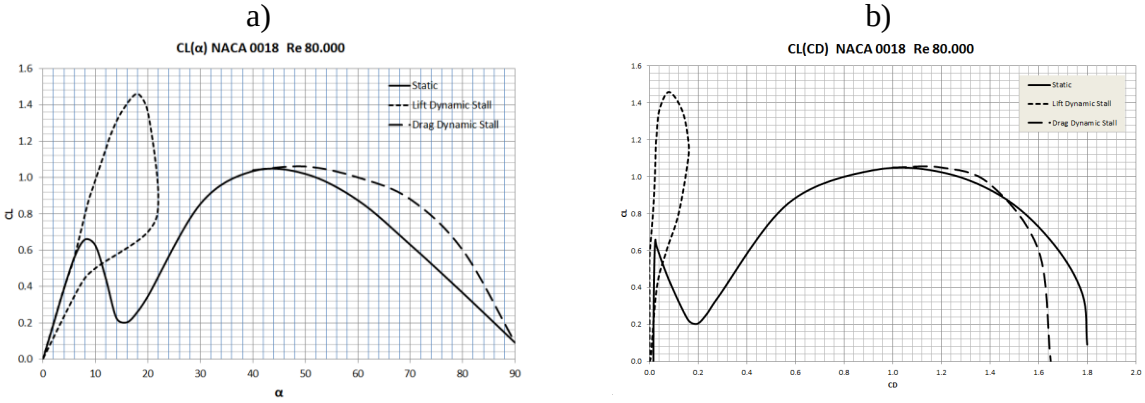

Figure 3: Static and dynamic lift and drag coefficients of NACA 0018 airfoil at R_{ec}=80000: a) $C_L(\alpha)$; b) $C_L(C_D)$.

The first phenomenon is a lift dynamic stall similar to the airfoils rapidly pitching with the angle of attack α, significantly beyond the static stall angle, α_{1ss} and normally can generate a substantially larger lift than can be obtained quasi- statically. This phenomenon is well documented [2], [3] and results from the combination of the unsteady motion of the airfoil and the separation of the boundary layer, when the stall process can be divided into four key stages; i.e. attached flow, development of the leading-edge vortex, post-stall vortex shedding, and the reattachment of flow. Therefore, in the present paper, we only focus on the Darrieus motion of confined airfoil blades at low TSR which experience high values of the angle of attack, $\alpha_D \ge 45^0$ and can trigger the drag dynamic stall phenomenon .The drag dynamic stall, little influenced by Reynolds number ,occurs only on blades operating in a confined flow filed , in which the rotor is acting as a pump on the separated volume of air forcing it to move radial towards the blade .In contrast to drag stall, the lift dynamic stall is very similar to the pitching motion of the both single airfoil blade and confined blade.

The drag dynamic stall is a term used to describe the delay in the drop of the second static stall lift coefficient, $C_{L_{2SS}}$ on the blade passing in the downwind ($\theta \cong 180^0$) and which can generate simultaneously little lift and significant drag reduction a short period of time at when TSR is of order unity.

The drag dynamic stall, occurring at low TSR in the range of λ=0.7-1.5 characterizes the shift of the operating modes from mixed lift–drag driving to full lift driving which is

important for the continuous acceleration of the rotor and its self starting. Though this phenomenon is very important for capability of the VAWTs to exceed the wind speed (i.e. TSR > 1), without extra components, it has not been identified in the wind turbine community. They have perceived the issue specially by its failure when some researchers have heuristically stated the inability of Darrieus type VAWTs with low solidity to self-start at low Reynolds number [4], [5]. The drag dynamic stall occurring at TSR of order unity belongs, by its nature, to the non-viscous flow (with little Reynolds number influence), while the lift dynamic stall, entails viscous events, mostly depended on Reynolds number. Besides, at high Reynolds numbers, the drag phenomenon is still alleviated by turbulence and its effect generated by the rough incidence change can be hidden by the blade-vortex interaction occurring pairs of shed leading-trailing vortices all along the leeward movement of the blade. These vortices of viscous wake observed both experimentally [6] or computationally [7], differ essentially from the stationary structure of counter-rotating potential- like vortex doublet, identified computationally by us in the vicinity of the up-downwind passage when TSR is about unity. For the drag stall process we have devised a two step aerodynamic scenario beginning with the formation of the potential vortex doublet which models the discontinuous incidence change at the up-downwind passage ($\theta = 180^0$) of the blade for $\lambda = 1$, and then followed by the superposition of the potential vortex structure, a parallel main stream (wind) and the blade rotation, which result in an interesting flow pattern with a stationary vortex doublet. This entity embedded in the flow field plays the role of "focus" which squeezes the streamlines around the airfoil when it passes across form upwind to downwind and modifies the separation of the boundary layer on upper surface (Fig.4).

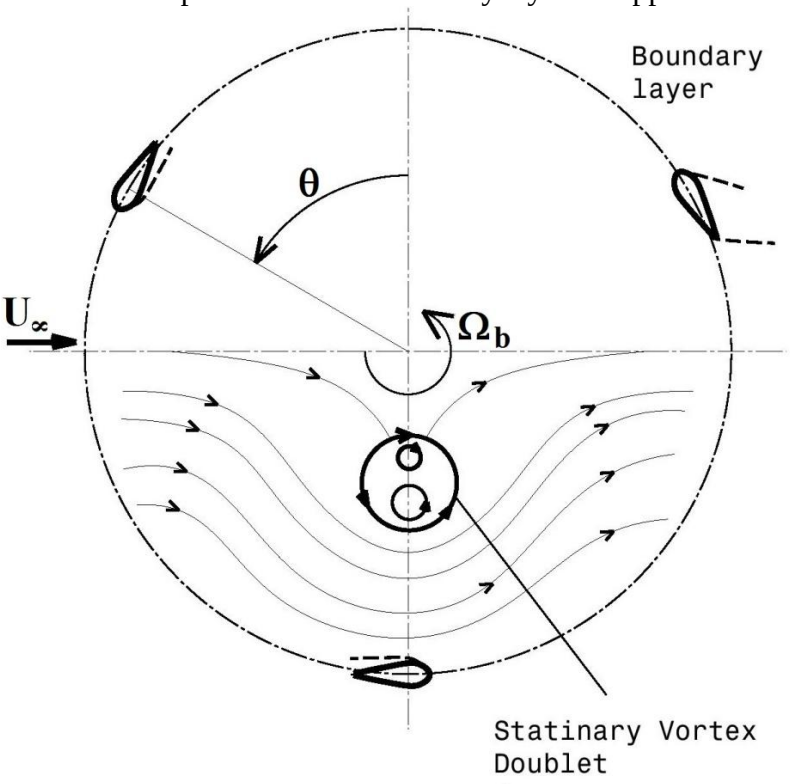

Figure 4: Flow pattern produced by a stationary vortex doublet in a parallel main stream and the Darrieus motion.

The nonviscous flow step of the scenario is followed by a viscous-flow step related to the gradual reduction of the volume of the separated boundary-layer flow on the upper side of the airfoil, forcing it to move chord-wise towards the trailing edge. The reduction of the volume of the separation bubble produces a pressure drop along the suction side increasing, thus, the blade loading. Thus, the rough switch of the angle of attack at $\lambda = 1$ becomes a smooth process via boundary layer which has the ability to accommodate to the pressure variation imposed by the inviscid flow.

Figure 4 illustrates the mechanism of dynamic stall resulting in the continuous lift producing at low tip speed ratios. However the exploitation of the high unsteadiness at $\lambda \cong 1$, to trigger this mechanism and further the acceleration up to λ=3 is directly related to rotor configurations: number of blades, chord-to-diameter ratio or their product (solidity σ) and blade aspect ratio. Therefore, for Re_c (based on chord length) and airfoil profile chosen the self starting can be achieved through a proper combination of these parameters.

3 START OF A VAWT

The wind experienced by the airfoil has two components: the wind in the rest frame, U_∞, and the relative wind induced by the motion of the blade, $\Omega_b R$.

The angle of attack α_D is then a function of magnitudes of U_∞ and $\Omega_b R$, and the azimuthal position θ (Fig. 1b). θ is also the angle between the oncoming wind and the tangential velocity of one blade.

Airfoils are typically defined in terms of lift and drag coefficients, with drag being parallel and lift perpendicular to the effective velocity perceived by the blade, U_{eff}. In this case it is more useful to define a thrust coefficient C_T which is the force acting tangentially

$$C_T = C_L(\alpha_D, \mathrm{Re}_c, k)\sin\alpha_D - C_D(\alpha_D, \mathrm{Re}_c, k)\cos\alpha_D, \tag{3}$$

where the lift and drag coefficients depend on the angle of attack, Reynolds number and reduced frequency. Thus, with the blade defined by a table of the static values $C_T(\alpha_D, \mathrm{Re}_c)$ over the full 360^0 range, it is simple to calculate torque and acceleration given by the parameters $\lambda(U_\infty, \Omega R)$ and θ. The total torque that the blade generates at any tip speed ratio can be obtained by integrating C_T over the azimuth angle ($C_m = \int C_T R d\theta$). But, the torque predicted in this way differs from the measured values [5], [8]. The results have shown that the quasi-steady torque (without unsteadiness induction) is in good agreement up to λ of around 0.5, afterwards the reduced frequency is high and the quasi-steady assumption becomes invalid. The quasi-steady prediction of C_T becomes negative [4] and the net torque produced by a blade around one revolution C_{m1} is negative at low TSR and the machine will not go faster.

If the torque is positive, the turbine is able to rotate independently and produce power; if the torque is negative, the turbine needs extra power to able to rotate. The positive value of experimental torque confirms that the unsteadiness can be exploited to produce positive C_m in the region of negative torque, i.e. in the dead band region. This positive C_m can be obtained by increasing c/D ratio (Fig. 2c). It is then clear that the means to escape from the dead band is to promote unsteady thrust and to reduce rotor inertia. This can be achieved by properly sizing

the rotor configuration where the confined blade behaves differently from one which is isolated

3.1 Numerical Modeling

In order to model the start of a straight-bladed, fixed geometry rotor, the two-dimensional characteristics of airfoils are used to calculate the forces due to the oncoming wind. A number of simplifications have been made, most notably neglecting induced flow and all dynamic effects concerning the lift force. Since at start when the angle of attack is higher than 45^0, the unsteady effects contribute more to drag reduction than to lift increment, these are taken into account naturally as a bulk unsteady effect into the drag coefficient

$$C_{Dun} = C_{Ds}(1-k), \tag{4}$$

Assuming that no power is extracted during starting and that the rotor torque Q acts only to accelerate the blades, the starting is governed by the following equation [9]

$$\frac{d\lambda}{dt} = \frac{RQ}{JU_\infty}, \tag{5}$$

where J is the total rotational inertia, Q is the driving torque and R is the rotor radius. By stepping through the azimuthal angle, the total torque can be integrated over a rotation at particular values of λ. Finally, the time-stepping predicts the resultant behavior due to specified initial conditions.

Figure 5 compares the starting performance of a three-bladed rotor with different levels of unsteadiness for Re_c = 80,000 and NACA 0018 airfoil. This shows that the increase of unsteadiness leads to a reduced idle running period, i.e. after the rotor has spin, the improved self-starting is provided by aerodynamic performance of the rotor.

a) b)

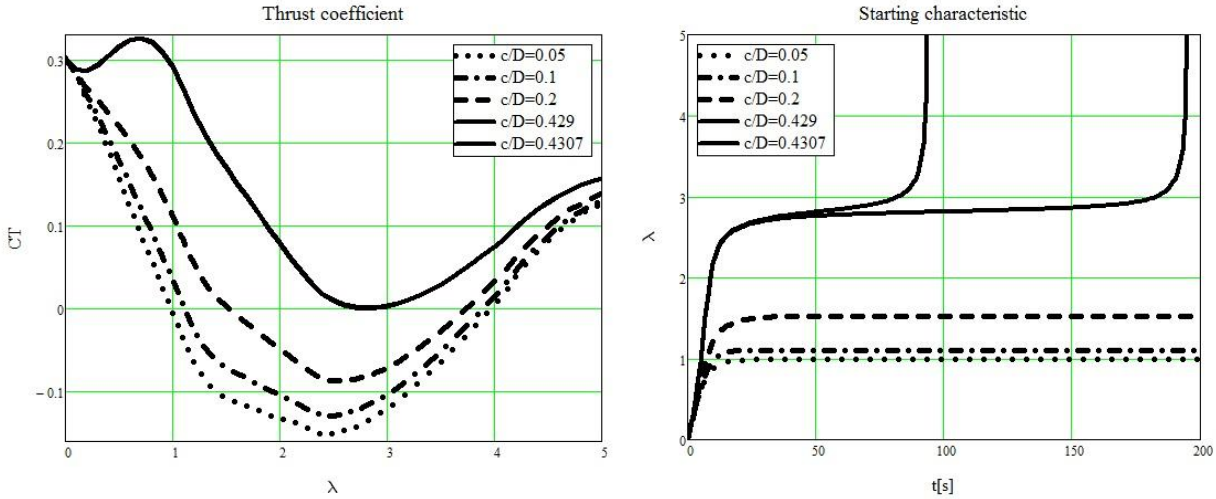

Figure 5: Effect of unsteadiness parameter (c/D) on starting performance: a) thrust coefficient; b) starting characteristics.

4 CONCLUSIONS

A physical description of Darrieus turbine starting capability has been investigated through a natural process occurring in Darrieus motion when the angle of attack roughly switches its direction at TSR = 1.0. The study of the Darrieus motion leads to the following conclusions:

1. A dynamic stall type, indentified on confined blades into a rotor at high angles of attack produces significantly drag reduction when TSR is of order unity. It is then called drag dynamic stall.
2. The drag dynamic stall promotes the shift of operating modes of VAWTs from mixed lift-drag mode to full lift mode and thereby produces the continuous thrust production when TSR exceeds the value of $\lambda = 1.0$.
3. The onset of the drag dynamic stall is determined by a level of unsteadiness inside rotor, which however is not a guarantee of further acceleration and it is possible the rotor will be locked in the dead band $(1 \le \lambda \le 1.5)$ due to a large area of high angle of attack and insufficient thrust production. In this case others parameters as blade thickness and turbine solidity can be altered for overcoming this drawback.

Besides the specified initial conditions (Reynolds number and airfoil profile), exploitation of the unsteadiness to promote self-starting can be achieved through a proper sizing of rotor configuration

ACKNOWLEDGMENT

This work was realized through the Partnership programme in priority domains – PN II, developed with support from ANCS CNDI – UEFISCDI, project no. PN-II-PT-PCCA-2011-32-1670.

REFERENCES

[1] Allet, A., Halle, S. and Paraschivoiu, I., *Numerical simulation of dynamic stall around an airfoil in Darrieus motion*, Journal of Solar Energy, **121**, (1999), 69-76.

[2] Wernert, P., Geissler, W., Raffel, M. and Kompenhans, J., *Experimental and numerical investigations of dynamic stall on a pitching airfoil*, AIAA J, **34** (5), (1996) 982-989.

[3] Wang, S., Ingham, D. B., Ma Lin, Pourkashanian, M. and Tao Zhi, *Numerical investigations on dynamic stall of low Reynolds number flow around oscillating airfoils*, Computers & Fluids, **39**, (2010) 1529-1541.

[4] Baker, J. R., *Features to aid or enable self starting of fixed pitch low solidity vertical axis wind turbines*, Journal of Wind Engineering and Industrial Aerodynamics (1983), **15**, 369-380.

[5] Hell, N., Dominy, R., Ingram, G. and Dominy. J., *Darrieus turbines: the physics of self-starting*, Proceedings of the Institution of Mechanical Engineers, Part A: Journal of Power and Energy, (2009), **223**, 21-29.

[6] Fujisawa, N. and Shibuya, S., *Observations of dynamic stall on Darrieus wind turbine blades*, Journal of Wind Engineering and Industrial Aerodynamics, (2001), **89**, 201-214.

[7] Ferreira, C. J. S., van Zuijlen, A., Bijl, van Bussel, H., G. and van Kuik, G., *Simulating dynamic stall in a two-dimensional vertical-axis wind turbine: verification and validation with particle image velocimetry data*, Wind Energy, (2010), **13**, 1-17.

[8] Chua, R. L., *Darrieus wind turbine analysis*, http://www.wind-turbineanalysis.netfirm.com, (2002).
[9] Wood, D., *Small Wind Turbines: analysis, design and application*, Springer-Velag London Limited, (2011).
[10] Dumitrescu, H., Dumitrache, Al., Frunzulica, F., Pal, A. and Turbatu, V., *TORNADO concept and realisation of a rotor for small VAWTs*, INCAS Bulletin, (2013), **5**, (3), 69-75.